Electronic Supplementary Information (ESI)

In-situ electrochemical characterisation of graphene and various carbon-based electrode materials: an internal standard approach

Dale A. C. Brownson, Peter J. Kelly and Craig E. Banks*

Faculty of Science and Engineering, School of Science and the Environment, Division of Chemistry and Environmental Science, Manchester Metropolitan University, Chester Street, Manchester M1 5GD, UK.

*Corresponding author:
Email: c.banks@mmu.ac.uk; Tel: ++(0)1612471196; Fax: ++(0)1612476831
Website: www.craigbanksresearch.com

Experimental details

For employment of the graphene working electrodes an electrochemical cell was utilised as described previously by our group. [1] Essentially, the various chemical vapour deposition (CVD) grown graphene films were deposited on Si/SiO_2 chips/wafers, which were then secured into a polytetrafluoroethylene (PTFE) housing unit with a silicone O-ring defining the working surface (diameter, 4.9 mm) and a steel contact making connection to the back of the chip, which *via* the use of silver conductive paint (applied to cover the back and sides of the chip in their entirety) ensures electrical conductivity from the front 'working surface' of the electrode to the electrode connector (to which a lead for the working electrode can be attached). Figure ESI-1 details the experimental set-up, adapted specifically for electrochemical measurements utilising CVD grown graphene. This unique cell design ensures that graphene is the only electrochemically active surface that is in contact with the solution during electrochemical measurements and allows the

direct electrical wiring of the graphene – but without worry that the connecting silver conductive paint might be exposed to the solution giving rise to false voltammetry. Using this electrochemical cell, the exposed working electrode area is consistently 0.189 cm^2 for all graphene samples studied.

The commercially available CVD synthesised monolayer graphene film was obtained from 'Graphene Supermarket' (Reading, MA, USA) [2] and is known as 'Monolayer Graphene on 285 nm SiO_2 Wafer'. The single layer continuous graphene film (*ca*. 97% graphene coverage (95% monolayer) with occasional holes, cracks and small multi-layer islands) comprises graphene grains of different crystallographic orientations (polycrystalline in nature) and is grown utilising a copper foil (25 μm thick) catalyst *via* a CVD synthesis method (*ca*. 1000 °C (cooling rate 40–300 °C min^{-1}) with H_2/CH_4 precursor (0.06 sccm and partial pressure 66.7 Pa) for less than 3 minutes growth time). [3-5]

The commercially available CVD synthesised *quasi*-graphene film (few-layer graphene film) was obtained from 'Graphene Supermarket' (Reading, MA, USA) [2] and is known as 'Multilayer Graphene on 285 nm SiO_2 Wafer'. The multi-layer (or few-layer) continuous graphene film (*ca*. 95% graphene coverage with occasional holes and cracks) comprises graphene grains of polycrystalline nature. The multi-layer graphene film is not uniform, which is evident through observation of the optical microscopy image depicted in Figure ESI-4B where a 'patchwork' like appearance indicates 'patches' of different thicknesses; the thickness varies from 1 to 7 layers, with an average of 4 graphene layers (the graphene layers within the same 'patch' are aligned relative to each other (there is a graphitic AB-stacking order)). [2] The multi/few-layered continuous graphene film is grown utilising a nickel foil (500 nm thick) catalyst *via* a CVD synthesis method (*ca*. 1000 °C (cooling rate 100 °C min^{-1}) with CH_4 precursor (10 sccm (H_2, 1400 sccm), ambient pressure) for *ca*. 5 minutes growth time). [3, 5, 6]

The commercially available CVD synthesised double-layer graphene film was obtained from 'Graphene Supermarket' (Reading, MA, USA) [2] and is known as 'Single/Double Layer Graphene on 285 nm SiO_2 Wafer'. The mono-/bi-layer continuous graphene film (*ca*. 95% graphene coverage (up to *ca*. 30% coverage is double-layer graphene islands) with occasional holes and cracks) comprising graphene grains of different crystallographic orientations (polycrystalline in nature) is grown utilising a modified method of the aforementioned CVD process. For example, a copper foil (206 nm thick) catalyst is utilised *via* a CVD synthesis method

(*ca*. 800 °C (cooling rate 40–300 °C min^{-1}) with H_2/CH_4 precursor (5 sccm and partial pressure 20 Pa) for *ca*. 10 minutes growth time). [3]

Following growth of the various graphene films, such films were transferred onto an oxidised silicon wafer (electrochemically inert supporting substrate) *via* a poly-methyl methacrylate (PMMA) assisted transfer method, as previously reported and characterised; [3, 4, 7-9] however, the exact details are proprietary information. [2] Note that other than securely 'housing' the CVD grown graphene chips/electrodes into the appropriate 'housing' unit prior to electrochemical measurements, the graphene films were used as-received from the supplier without any further modification. The graphene 'wafer' macrostructures, before being adapted into electrodes using the 'electrode 'housing cell/unit', are 1 × 1 cm^2 in size. The manufacturer reports a resistivity of *ca*. 660–1500 and 500–1500 Ω/□ across the lateral surface of the monolayer- and *quasi*- graphene wafers respectively. [2] Attempts were made to independently measure the resistivity; however, due to the fragile nature of the graphene surfaces we were unable to ascertain a reliable/reproducible response.

Atomic force microscopy (AFM) data was collected in TappingMode™ using a Veeco Dimension 3100 scanning probe microscope with a NanoScope V controller; images were produced using NanoScope analysis v1.4. Raman spectra were recorded using LabRam (Jobin-Ivon) with a confocal microscope (×100 objective) spectrometer with a He-Ne laser at 633 nm excitation at a very low laser power level (0.9 mW) to avoid any heating effect (beam width *ca*. 100 μm). X-ray photoelectron spectroscopy (XPS, K-Alpha, Thermo Scientific) was used to analyse the chip surface. All spectra were collected using Al-K radiation (1486.6 eV), monochromatised by a twin crystal monochromator, yielding a focused X-ray spot with a diameter of 400 μm, at 3 mA × 12 kV. The alpha hemispherical analyser was operated in the constant energy mode with survey scan pass energies of 200 eV to measure the whole energy band and 50 eV in a narrow scan to selectively measure the particular elements. Thus, XPS was used to provide the chemical bonding state as well as the elemental composition of the surface. Charge compensation was achieved with the system flood gun that provides low energy electrons and low energy argon ions from a single source.

Graphene Characterisation

Below we report the physicochemical characterisation of our various graphene samples. Note that batch characterisation has been performed (as is common practice in the literature) and thus the characterisation presented is taken as representative with respect to the electrodes utilised throughout this research.

We first consider the structural characterisation of the monolayer and few-layer (termed *quasi*-graphene) CVD grown graphene materials *via* AFM analysis. Figures ESI-2A and ESI-2B depict the resultant AFM images of the monolayer CVD grown graphene macrostructure. It is evident that the graphene domains comprising the material consist predominantly of single-layer graphene sheets, which appear to exhibit an intra-planar microcrystalline size, L_a of between 500 and 5000 nm and an average inter-planar microcrystalline size, L_c of *ca*. 0.34 nm (one monolayer), which compares well to pristine graphene as reported theoretically in the literature. [10] The optical image in Figure ESI-3B highlights occasional holes in the continuous monolayer graphene film and also reveals the presence of occasional small few-layer graphitic islands on the graphene surface. Closer inspection of the AFM images depicted in Figure ESI-2 reveals the presence of ripples/wrinkles at the grain boundaries of the monolayer graphene domains, which are an inherent property of CVD grown graphene. [3] Figures ESI-2C and ESI-2D depict the respective AFM images of the CVD grown *quasi*-graphene macrostructure (few-layered graphene). It is evident that the graphene domains comprising the surface possess average L_a values similar to those observed for the monolayer graphene alternative (*vide supra*); however, in this case it is clear that the graphene material consists of a single-/few- layer graphene support film (which as above is continuous, with occasional holes, cracks and ripples occurring at grain boundaries, see Figure ESI-4B also) over which large few-layer graphitic domains (graphitic islands) are distributed across the surface. These multiple layers of stacked graphene sheets, so-called graphitic islands, [11] result in the few-layer graphene domains/islands possessing large L_c values (L_c ranges from *ca*. 0.34 to 2.38 nm, *i.e*. 1–7 layers with an average of 4 graphene layers); however, such values do not correspond to the structural characteristics of graphite [12, 13-15] and thus the composition of the CVD grown few-/multi- layer graphene electrode is consistent with that expected for *quasi*-graphene. [16, 17]

Raman spectroscopy was next performed on the graphene macrostructures. Figure ESI-3A depicts the Raman spectrum of the ‘monolayer’ graphene film in addition to an

optical micrograph (Figure ESI-3B) of the probe position upon the domain surface. The Raman spectrum reveals two characteristic peaks at *ca*. 1550 and 2680 cm^{-1}, which are due to the G and 2D (G') bands respectively. Note that the highly symmetrical 2D (G') peak indicates that the surface is comprised of single-layer graphene (consistent with AFM and optical images, *vide supra*). [13-15] The full width at half-maximum (FWHM) of the 2D band is found to be 29.1 cm^{-1}, corresponding in the literature to that of single layer graphene. [18] Additionally, the intensity ratio of the G and 2D bands (G/2D = 0.37) indicates that the graphene electrode is indeed comprised principally of single-layer graphene domains, where the low intensity of the G band in relation to the 2D peak is characteristic of monolayer graphene. [13-15] The presence of a small D band (1330 cm^{-1}) indicates a small number of structural defects on the graphene surface (limited basal plane crystal defects), however the relatively low intensity of the D band, which is not easily distinguishable from the 'base line', suggests that an ordered graphene structure is present which is of high quality and thus represents that of pristine graphene in nature. [13-15] Figures ESI-4A and ESI-4B depict the respective optical micrograph and Raman spectrum of the 'few-/multi- layered' (*quasi*-) graphene film. The Raman spectrum reveals the two characteristic peaks (G and 2D (G')) of graphene/graphitic materials at *ca*. 1550 and 2680 cm^{-1}. [13-15] The high symmetry of the 2D (G') band peak, indicates that the surface comprises single- to few- layer graphene sheets (the slightly broader peak signifies the presence few-layer graphene, [18] which is consistent with AFM and optical images, *vide supra*). Note that the 2D peak does not indicate the presence of graphite, which is characterised by a non-symmetrical, broad peak with distortion evident in the form of a 'shoulder'. [13-15] The FWHM of the 2D band is found to be 56.2 cm^{-1}, corresponding in the literature indeed to that of few layer graphene. [18] In this case the intensity ratio of the G and 2D bands (G/2D = 1.22) also indicates the presence of few-layered graphene domains, with the relatively equal intensities of the G and 2D peaks coinciding with the presence of *ca*. 3 or 4 graphene layers (for this probe position), [13-15] which again is consistent with that expected for the structural configuration of *quasi*-graphene. [16, 17] The low/faint intensity of the D band (1315 cm^{-1}) again suggests that in this case the *quasi*-graphene is of high quality and pristine in nature, possessing a low level of basal plane crystal defects across its lattice. [13-15] Note that increasing the number of graphene layers towards the structural composition of graphite would result in evolution of the G peak intensity such that it would significantly surpass that of the 2D peak, characterised by G/2D ratios exceeding 3.75 (in addition to the emergence of the 'shoulder' effect

noted above); thus it is clear that none of the graphene samples utilised in this study display similar structural characteristics relating to graphite, rather single, double and few layered graphene structures.

Figures ESI-3 and ESI-4 also depict Raman maps that were obtained over a relatively large central area of the graphene surfaces in order to ascertain the overall quality of the graphene present on the monolayer graphene (Figure ESI-3) and *quasi*-graphene (Figure ESI-4) materials. The Raman maps are in excellent agreement with analysis obtained *via* the individual Raman probe positions and with the AFM images. Figures ESI-3C and ESI-4C represent variations in the intensity of the 2D/G peak ratios over the area analysed on the monolayer and *quasi*-graphene samples respectively, with the darker spots (relative to the scale provided) indicating thicker graphene regions. It is evident that the 'monolayer graphene' indeed comprises a single-layer continuous graphene film (indicated by the uniform distribution of 'lighter pixels') with occasional defects or islands present (*i.e.* the darker spots in Figure ESI-3C). In contrast the *quasi*-graphene ('few-layered graphene') possesses a large number of apparent multi-layered islands distributed across the surface, each with varying thickness as indicated by the severe contrast observed between multiple 'light' and 'dark' patches (Figure ESI-4C). Figures ESI-3D and ESI-4D represent variations in the Full Width at Half Maximum (FWHM) of the 2D peak over the areas analysed on the monolayer and *quasi*-graphene surfaces respectively. The width of the 2D peak is related to the quality of the graphene present, where 'thinner' peak widths (darker pixels) indicate pristine single layer graphene and 'thicker' (more perturbed) peak widths (lighter pixels) are indicative of thicker graphene layers (as discussed earlier). The even distribution of colour in both maps (Figures ESI-3D and ESI-4D) indicates pristine graphene is present on both samples, however relative to the scale provided, the 'darker' colouring of the map representing the monolayer graphene (Figure ESI-3D) is indicative of single-layer graphene relative to the 'lighter' colouring of the quasi-graphene indicating the presence of multi-layered graphene.

Finally (for the case of the monolayer and few-layered graphene samples), XPS was conducted on the two graphene materials. De-convolution of the spectra relating to the monolayer graphene domain revealed it to be composed of 42.73 % carbon, 27.72 % oxygen and 29.55 % silicon. The carbon content comprises of 32.15 % corresponding to 284.8 eV which is characteristic of graphitic groups, and 10.27 % at 286.6 eV which corresponds to C–O and C=O bonds. Of the oxygen content, 2.1 % is comprised from contributions at 287.9 and 533.15 eV,

which correspond to C=O and C–O groups. Note that contributions from the silicon (29.55 %) and remaining oxygen content (25.62 %) are a result of the probe depth (*ca*. 2–3 nm) given that the thin graphene film is supported on top of an oxidised silicon wafer. In considering only the carbon and oxygen contributions arising from the graphene material (which are exposed only to the solution when used in electrochemistry), XPS reveals the monolayer graphene to comprise a O/C ratio of *ca*. 0.05, which is consistent with that of a low oxygen content of the graphene domain and thus is pristine in nature. De-convolution of the spectra relating to few-layered graphene (*quasi*-graphene) revealed it to be composed of 61.50 % carbon, 20.06 % oxygen and 18.44 % silicon (note that due to the probe depth (*vide supra*) and the increased thickness of the multi-layered graphene surface, in this case the % contribution of carbon has increased and the respective % contribution of silicon has decreased; as expected). The carbon content comprises of 45.62 % corresponding to 284.6 eV which is characteristic of graphitic groups, and 8.05 and 6.64 % at 285.7 and 286.9 eV respectively which correspond to C–H, C=C, C–O and C=O bonds. In this case, of the oxygen content 4.4 % is comprised from contributions at 287.9 and 533.15 eV. As above, the silicon (18.44 %) and the remaining oxygen content (15.66 %) contributions are a result of the probe depth utilised (which penetrates the support surface). For the case of the *quasi*-graphene, considering only the carbon and oxygen contributions arising from the graphene material XPS reveals a O/C ratio of *ca*. 0.07, which is consistent with inferences gained through Raman spectroscopy and indicates that the *quasi*-graphene structure is comprised of pristine graphene domains.

Next, we investigate the physicochemical properties of the double-layered defect abundant graphene material. AFM images of the double-layer graphene macrostructure are shown in Figure ESI-5. It is evident that the graphene domains comprising the material possess a large number of surface defect sites, where ‘cracks’ are observable between/throughout the double-layer graphene domains. Also evident is the distinction between the AFM images of the monolayer graphene (Figures ESI-2A and ESI-2B) and this two-layer sample (Figure ESI-5), with the latter possessing a ‘bulky’ topography (*i.e.* wrinkles and ripples characteristic of single-layer graphene are absent in the double-layer graphene). Raman spectroscopy of the double-layer graphene is shown in Figure ESI-6, revealing the two characteristic G and 2D peaks of graphitic materials at *ca*. 1580 and 2800 cm^{-1} respectively. As with the previous two graphene materials characterised (see earlier), the high symmetry of the 2D peak indicates the presence of pristine graphene. The

FWHM of the 2D band was found to be 32.3 cm^{-1}, corresponding to that of double layer graphene.[18] The intensity ratio of the G and 2D bands (G/2D = 0.86) evident in Figure ESI-6 indicates the presence of double-layered graphene domains given that the relatively equal intensities (with only a minimal reduction in the G peak relative to the 2D peak) coinciding with previous reports for two-layer graphene. AFM allows us to validate the overall quality of the graphene sample, which indeed confirms that the double-layer graphene macrostructure is comprised of a uniform two-layer graphene domain, on top of which occasional graphitic islands exist (see inset of Figure ESI-6). Also evident in Figure ESI-5 is an observable 'crack', which indicates the presence of an edge plane like- site/defect (*i.e.* a grain boundary).

Again, XPS was conducted on the double-layer graphene material. De-convolution of the spectra revealed a composition of 29.21 % carbon, 30.12 % oxygen and 39.06 % silicon. The carbon content comprises of 18.7 % corresponding to 284.5 eV which is characteristic of graphitic groups, and 8.73 and 1.78 % at 286.1 and 288.9 eV respectively which correspond to C–H, C=C, C–O and C=O bonds. Of the oxygen content, 0.82 % is comprised from contributions at 535.4 eV. The silicon (39.1 %) and the remaining oxygen content (29.3 %) contributions are a result of the probe depth utilised (which penetrates the support surface, see earlier). For the case of the double-layer defect-graphene, considering only the carbon and oxygen contributions arising from the graphene material, XPS reveals a O/C ratio of *ca*. 0.03.

In summary, we have fully characterised our graphene samples which have been fabricated *via* CVD and transferred onto an inert SiO_2 substrate utilising a PMMA transfer process. The monolayer graphene film comprises 97% single-layer graphene domains with occasional small multi-layered graphene islands and possesses a O/C ratio of *ca*. 0.05, indicating the presence of pristine monolayer graphene. The few-layered graphene (*quasi*-graphene) film comprises 95% graphene coverage with the thickness of individual graphene domains varying from 1 to 7 layers, with an average of 4 graphene layers (on top of which the multi/few-layered graphene islands are situated) and possesses a O/C ratio of *ca*. 0.07, indeed indicating the presence of *quasi*-graphene.[17] The double-layer graphene film shows it to be comprised of 95% graphene coverage, with an average thickness of two-layers across the graphene domains, however with a large number of structural defects/islands giving rise to a high global coverage of edge plane like- sites/defects.

Figure ESI-1

Schematic diagram of the CVD graphene chip 'housing' unit (A). Cross-sectional view of the assembled CVD grown graphene working electrode when fully incorporated (B) for exclusive use with the CVD grown graphene chips/substrates.

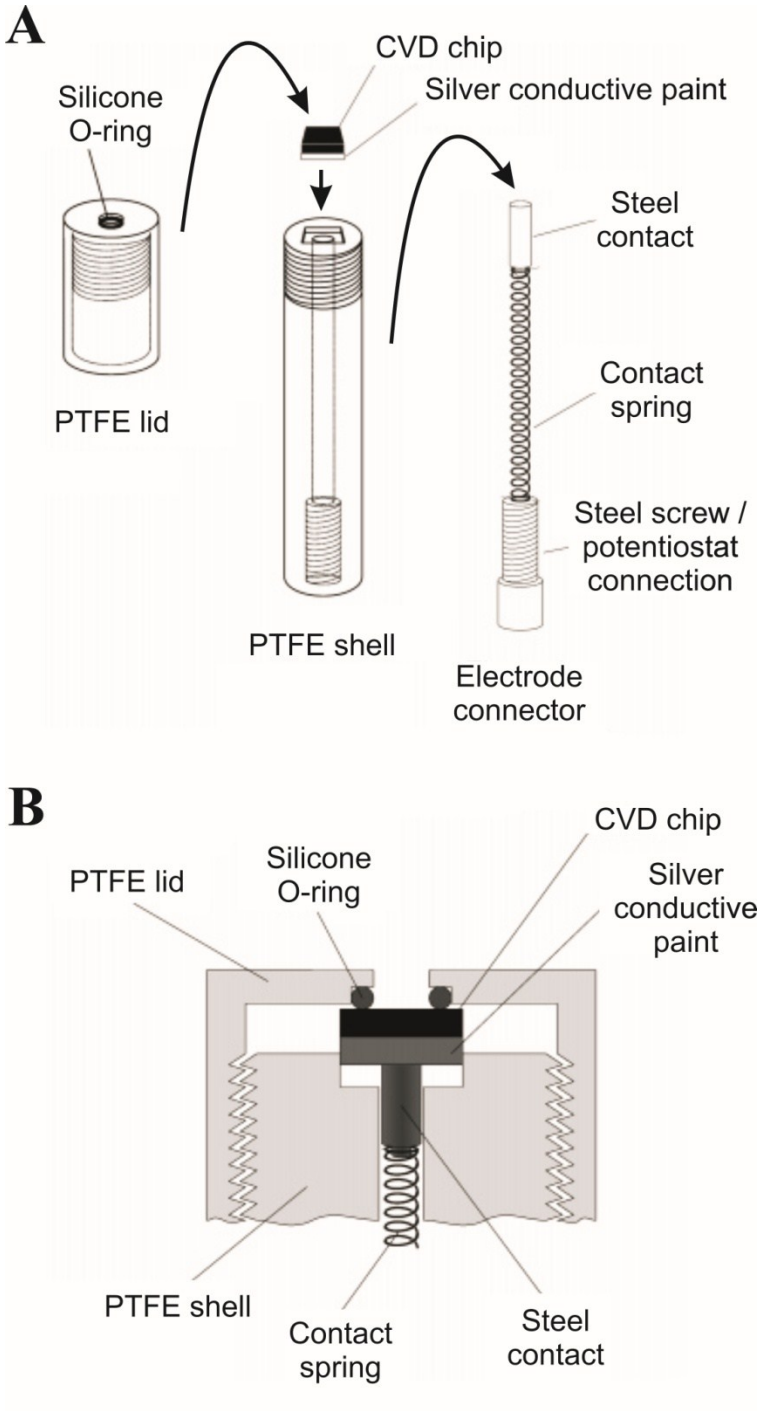

Figure ESI-2

AFM images of the monolayer graphene (A and B) and of the (few-layer) *quasi*-graphene (C and D). Successive images are progressively focused into the sample.

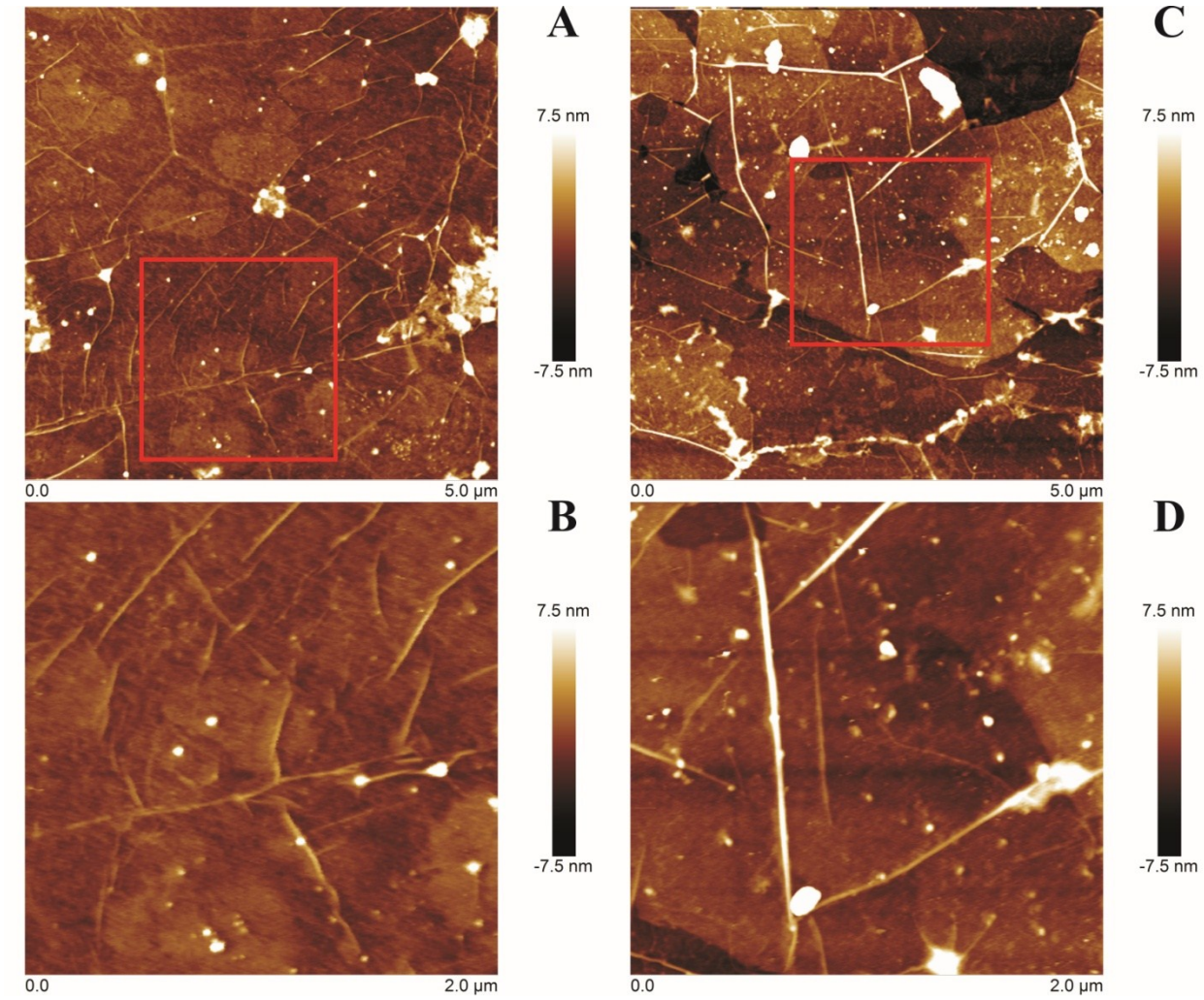

Figure ESI-3

Individual Raman spectroscopy characterisation of monolayer graphene (A). Raman maps and supporting optical micrographs indicating the sample area utilised (B, C and D). Raman maps show monolayer graphene: (C) 2D/G band ratio, where darker areas represent increased graphene layer numbers; and (D) the FWHM of the 2D peak, with lighter areas indicative of thicker graphene domains.

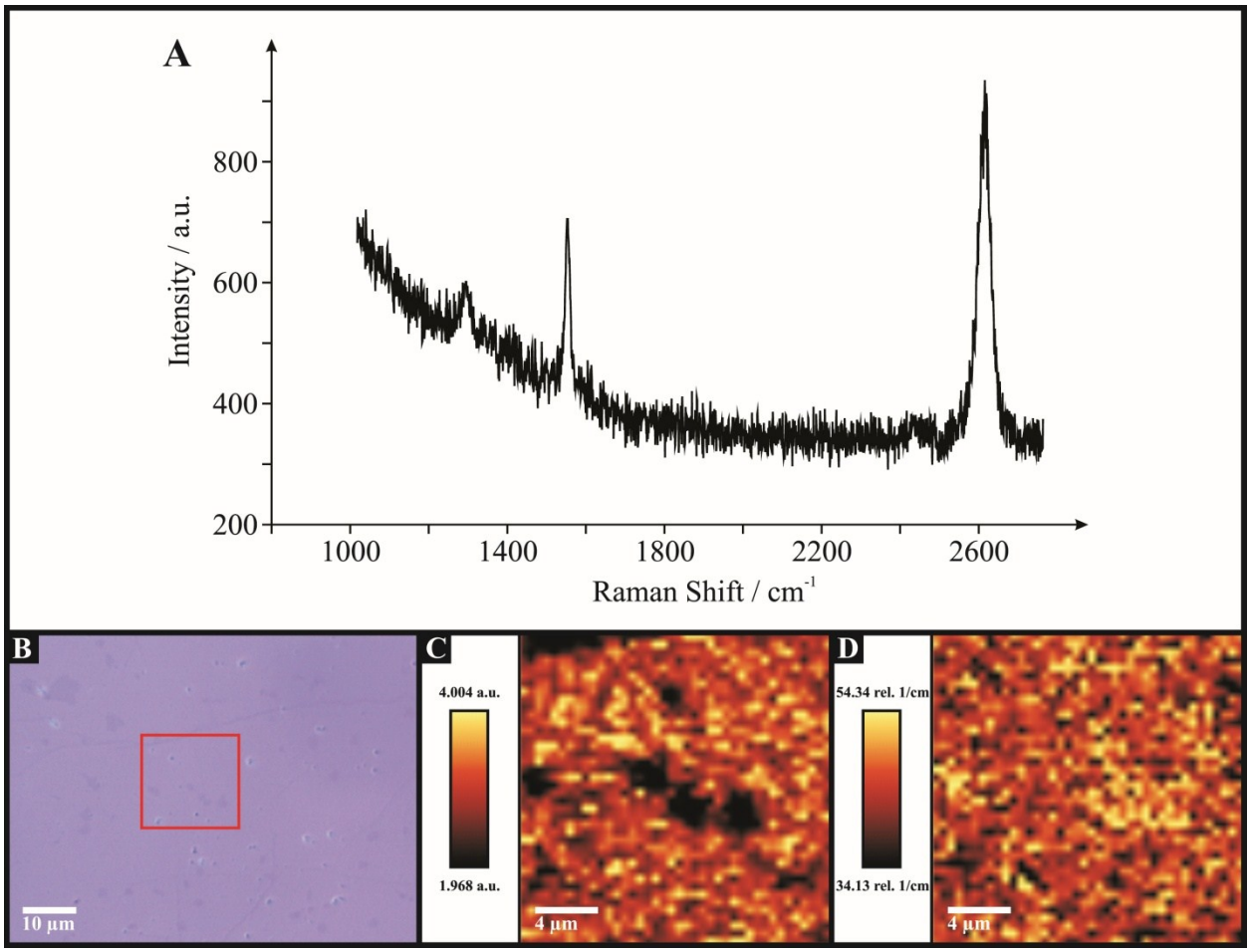

Figure ESI-4

Individual Raman spectroscopy characterisation of (few-layer) *quasi*-graphene (A). Raman maps and supporting optical micrographs indicating the sample area utilised (B, C and D). Raman maps show *quasi*-graphene: (C) 2D/G band ratio, where darker areas represent increased graphene layer numbers; and (D) the FWHM of the 2D peak, with lighter areas indicative of thicker graphene domains. Note that the dark spots on the optical micrograph (B) indicate stacked graphene layers/islands (few/multi-layers).

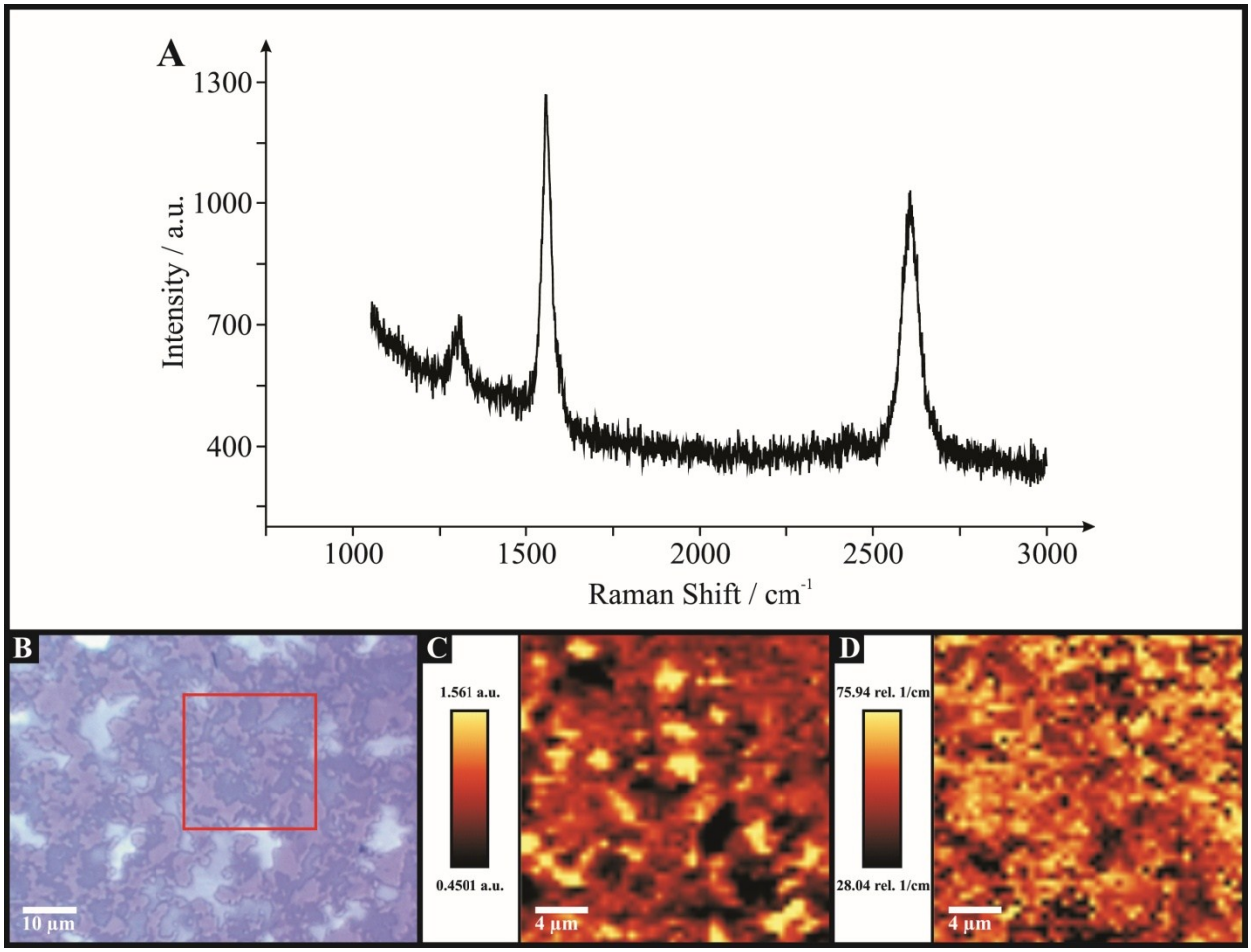

Figure ESI-5

AFM images of the double-layer defect-graphene, successive images are progressively focused into the sample.

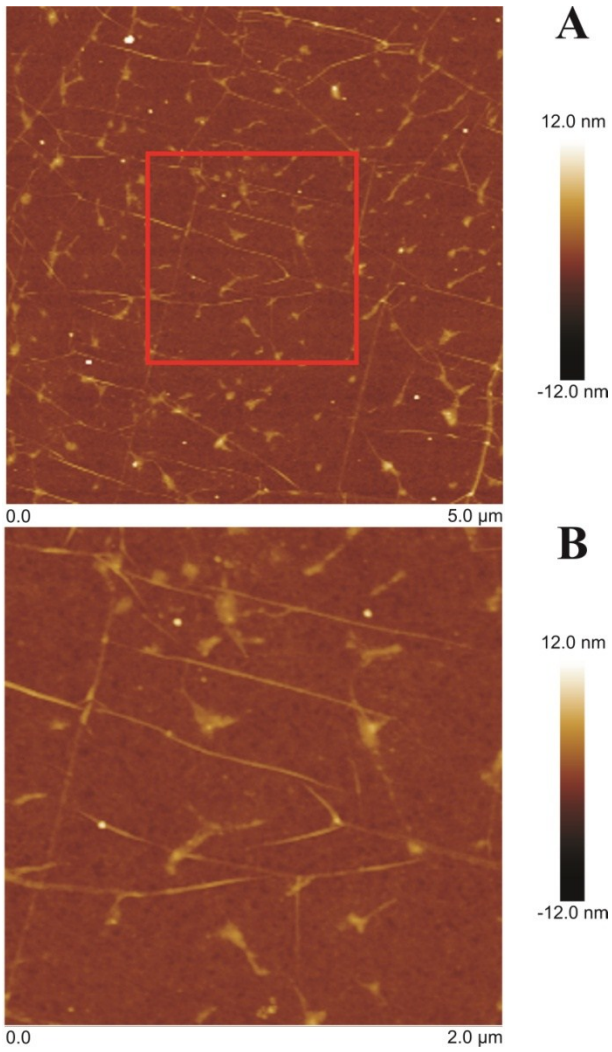

Figure ESI-6

Characterisation of the double-layer defect-graphene macrostructure. Raman spectroscopy, with an optical micrograph (inset) indicating the single probe position utilised.

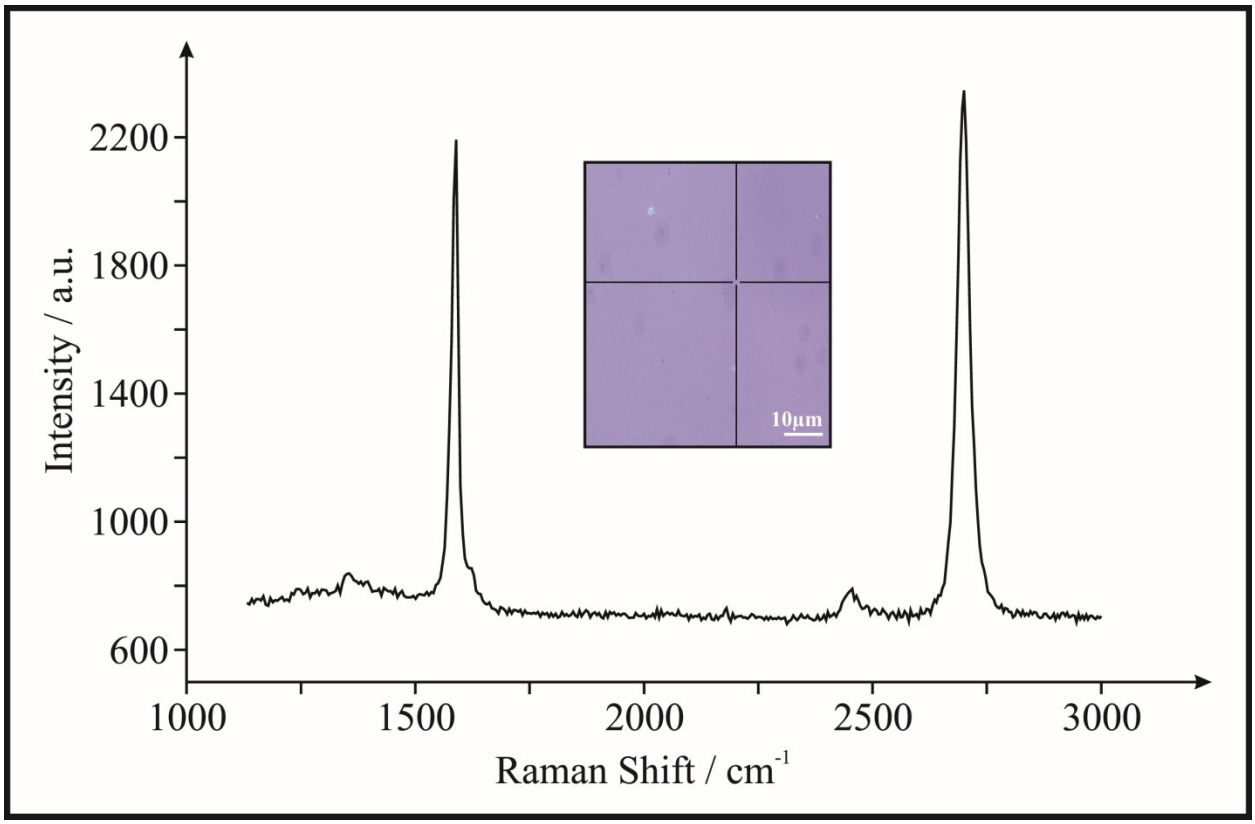

References

1. D. A. C. Brownson, R. V. Gorbachev, S. J. Haigh and C. E. Banks, *Analyst*, 2012, **137**, 833-839.
2. Graphene-Supermarket, http://www.graphene-supermarket.com (accessed 1st September 2014).
3. D. A. C. Brownson and C. E. Banks, *Phys. Chem. Chem. Phys.*, 2012, **14**, 8264-8281.
4. X. Li, W. Cai, J. An, S. Kim, J. Nah, D. Yang, R. Piner, A. Velamakanni, I. Jung, E. Tutuc, S. K. Banerjee, L. Colombo and R. S. Ruoff, *Science*, 2009, **324**, 1312-1314.
5. X. Li, W. Cai, L. Colombo and R. S. Ruoff, *Nano Lett.*, 2009, **9**, 4268-4272.
6. A. Reina, S. Thiele, X. Jia, S. Bhaviripudi, M. S. Dresselhaus, J. A. Schaefer and J. Kong, *Nano Res.*, 2009, **2**, 509-516.
7. X. Li, Y. Zhu, W. Cai, M. Borysiak, B. Han, D. Chen, R. D. Piner, L. Colombo and R. S. Ruoff, *Nano Lett.*, 2009, **9**, 4359-4363.
8. X. Liang, B. A. Sperling, I. Calizo, G. Cheng, C. A. Hacker, Q. Zhang, Y. Obeng, K. Yan, H. Peng, Q. Li, X. Zhu, H. Yuan, A. R. H. Walker, Z. Liu, L.-M. Peng and C. A. Richter, *ACS Nano*, 2011, **5**, 9144-9153.
9. M. Her, R. Beams and L. Novotny, *Phys. Lett. A*, 2013, **377**, 1455-1458.
10. D. A. C. Brownson, D. K. Kampouris and C. E. Banks, *Chem. Soc. Rev.*, 2012, **41**, 6944-6976.
11. D. A. C. Brownson and C. E. Banks, *Phys. Chem. Chem. Phys.*, 2011, **13**, 15825-15828.
12. A. G. Guell, N. Ebejer, M. E. Snowden, J. V. Macpherson and P. R. Unwin, *J. Am. Chem. Soc.*, 2012, **134**, 7258-7261.
13. D. Graf, F. Molitor, K. Ensslin, C. Stampfer, A. Jungen, C. Hierold and L. Wirt, *Nano Lett.*, 2007, **7**, 238-242.
14. A. C. Ferrari, *Solid State Commun.*, 2007, **143**, 47-57.
15. Y. Y. Wang, Z. H. Ni, T. Yu, Z. X. Shen, H. M. Wang, Y. H. Wu, W. Chen and A. T. S. Wee, *J. Phys. Chem. C*, 2008, **112**, 10637-10640.
16. D. A. C. Brownson, L. C. S. Figueiredo-Filho, X. Ji, M. Gómez-Mingot, J. Iniesta, O. Fatibello-Filho, D. K. Kampouris and C. E. Banks, *J. Mater. Chem. A*, 2013, **1**, 5962-5972.
17. D. A. C. Brownson and C. E. Banks, *The handbook of graphene electrochemistry*, Springer Publishing, London, U.K., 2014.
18. Y. Hao, Y. Wang, L. Wang, Z. Ni, Z. Wang, R. Wang, C. K. Koo, Z. Shen and J. T. L. Thong, *Small*, 2010, 6, 195-200.